Investigation of Polarization Effects on new Mask Materials

Karsten Bubke[1*], Silvio Teuber[1], Ingo Hoellein[1], Hans Becker[2**], Holger Seitz[2], Ute Buttgereit[2]
[1]Advanced Mask Technology Center GmbH & Co. KG, Raehnitzer Allee 9, D-01109 Dresden, Germany;
[2]Schott Lithotec AG, Jerusalemer Str. 13, D-98617 Meiningen, Germany

ABSTRACT

As microlithography moves to smaller critical dimensions, structures on reticles reach dimensions comparable to the operating wavelength. Furthermore, with increasing NA the angle of incidence of light illuminating the mask steadily increases. In particular for immersion lithography this will have severe consequences on the printing behavior of reticles. Polarization effects arise which have an impact on, for example, the contrast of the printed image. Angular effects have to be considered when aggressive off-axis illumination schemes are used. Whereas numerous articles have been published on those effects and the underlying theory seems to be understood, there is a strong need for experimental verification of properties of real masks at the actinic wavelength.

This paper presents measurements of polarization effects on different mask blank types produced at Schott Lithotec including chrome and alternative absorber binary mask blanks as well as phase shift mask blanks. Thickness and optical dispersion of all layers were determined using grazing incidence x-ray reflectometry (GIXR) and variable angle spectroscopic ellipsometry (VASE). The set of mask blanks was patterned using a special design developed at Advanced Mask Technology Center (AMTC) to allow measurements at different line width and pitch sizes. VUV Ellipsometry was then used to measure the properties of the structured materials, in particular the intensities in the 0^{th} and 1^{st} diffraction order for both polarization directions and varying angle of incidence. The degree of polarization of respective mask types is evaluated for dense lines with varying pitches and duty cycle. The results obtained experimentally are compared with simulations based on rigorous coupled wave analysis (RCWA).

Keywords: Polarization, high NA, immersion lithography, binary masks, high transmission masks

1. INTRODUCTION

With decreasing feature sizes in optical lithography the structures on the photomask reach dimensions comparable to the wavelength of the exposure system. As a result, topography effects have a significant influence on the diffraction properties of reticles[1]. This will become even more severe with the emergence of immersion lithography extending imaging to the sub-50nm regime[2-6]. The intensity distribution of the diffracted light will be substantially different from the case of an infinitely thin mask, which is often referred to as the Kirchhoff-approximation. Furthermore, the transmission through the mask will be polarization dependent[7]. As the interference of diffraction orders in the resist is substantially different for TE- (electric field vector is perpendicular to the propagation direction) and TM-components (magnetic field vector is perpendicular to the propagation direction), the mask can have a considerable impact on the imaging properties of the overall system. Furthermore, for hyper NA-systems the angle of incidence of light on the mask can have an influence on diffraction that needs to be taken into account, in particular when aggressive off-axis illumination schemes are used[8]. Finally, mask induced phase effects might lead to the introduction of additional aberrations. That means, the mask is not only carrying the structural information which is transferred to the wafer but acts as an additional optical element in the lithography system.

For an evaluation of the imaging properties of reticles all these effects must be taken into account. This requires first the accurate characterization of mask blanks with respect to layer structure and optical properties. Furthermore, an evaluation of the diffraction properties of structured mask materials is needed. To separate the influence of mask topography from effects arising from other elements in the lithography system, e.g. the projector optics, an experimental investigation of the diffracted light directly behind the reticle becomes important.

[*] karsten.bubke@amtc-dresden.com, phone +49 351 4048 377, fax +49 351 4048 9377
[**] hans-willy.becker@schott.com, phone +49 3693 522 328, fax +49 3693 522 101

In this paper we investigate polarization effects of new mask materials developed at SCHOTT Lithotec. The materials under investigation include a thin chrome absorber, a two layer phase shifting system which allows tuning of the transmission in a large range and finally an alternative binary absorber material with a low etch bias based on tantalum nitride. All materials are characterized using grazing incidence x-ray reflectometry (GIXR) and variable angle spectroscopic ellipsometry (VASE). For an evaluation of the diffraction properties of structured materials, the 0^{th} and 1st diffraction order of lines and spaces structures with different pitches and varying duty cycles are measured and compared with simulations based on rigorous coupled wave analysis.

The paper is organized as follows. In Section 2 the properties of the respective materials are discussed. Section 3 provides information about the mask design and patterning, Section 4 describes the experimental setup. In Section 5 the results of the polarization measurements are presented and compared with simulations. Finally, an estimation of the influence of polarization on the imaging performance is given.

2. CHARACTERIZATION OF NEW MASK MATERIALS

At SCHOTT Lithotec three different mask blanks were produced using ion beam sputter technology. Figure 1 shows a schematic drawing of the three layer designs. The first one on the left is the very thin dry etch optimized binary chrome absorber achieving an optical density of three at 248 nm with a thickness of 60 nm only. The two layer phase shifting system in the middle allows tuning of transmission from 6% up to 30% preserving a phase shift of 180°. The binary on the right is based on tantalum nitride as an alternative absorber material achieving almost zero etch bias.

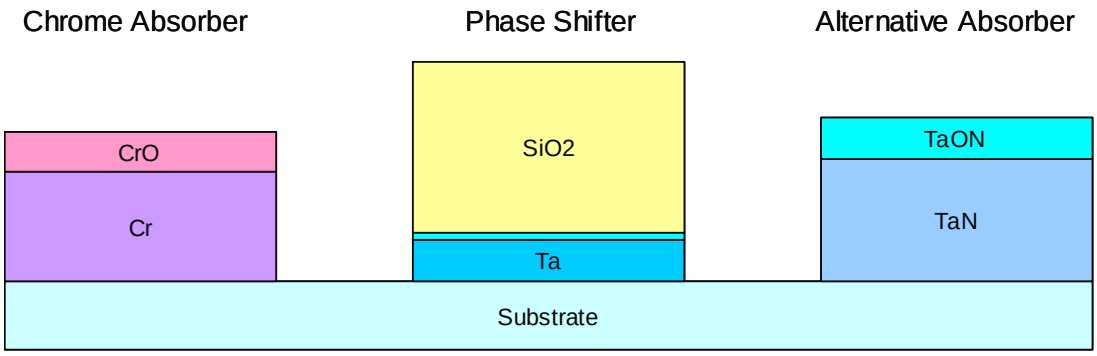

Figure 1: Schematic drawing of chrome absorber, phase shifter and alternative absorber layer designs.

For all three systems deposition parameters were optimized to combine very good dry etch capability with high uniformity of layer thickness and optical values. Especially the absorber layers can be made very thin taking advantage of the dense and compact layers provided by ion beam sputter technology. Layer thickness of the sputtered films were measured by grazing incidence x-ray reflectometry (GIXR). This method not only provides thickness information with sub nm resolution but also film density and interface roughness. Dispersion data were determined using a VUV-VASE® ellipsometer made by Woollam taking advantage of the already known layer thickness. The following tables contain detailed dispersion and design information for the three systems.
Table 1 contains the design of the chrome absorber. Thickness of the CrO antireflection layer is tuned to achieve a minimum reflection of 12% at 248 nm. Thickness of the Cr absorber layer is tuned to preserve an optical density above three for 248 nm and below. Since the film is very dense the total layer thickness can be reduced to 60 nm only.

Material	193 nm		257 nm		Thickness
	n	k	n	k	
Substrate	1.56	0.00	1.50	0.00	
Cr	1.12	1.95	1.36	2.73	48 nm
CrON	2.03	1.50	2.62	0.92	12 nm

Table 1: Dispersion data and layer thicknesses of the chrome absorber.

Table 2 contains the design of the tantalum/silica phase shifter. Thickness of the tantalum layer is tuned to achieve the desired transmission value, for this sample 20% transmission at 193 nm. Phase shift of the system is in first approximation linear with silica layer thickness which is adjusted to achieve a phase shift of 180°. In contact with oxygen tantalum builds a thin native oxide layer. For exact calculations this thin oxide layer has to be taken into account and the VUV-VASE® ellipsometric dispersion data are therefore included in the table.

Material	193 nm		257 nm		Thickness
	n	k	n	k	
Substrate	1.56	0.00	1.50	0.00	
Ta	1.63	2.58	2.25	2.67	10.6 nm
Ta2O5	2.11	1.27	3.04	0.47	1.5 nm
SiO2	1.63	0.006	1.56	0.001	152 nm

Table 2: Dispersion data and layer thicknesses of the tantalum/silica phase shifter.

Table 3 lists the design of the tantalum nitride alternative absorber. Thickness of the system is adjusted to achieve an optical density of 3 at 193 nm. This absorber is currently under development and especially layer thickness will be further reduced.

Material	193 nm		257 nm		Thickness
	n	k	n	k	
Substrate	1.56	0.00	1.50	0.00	
TaN	2.70	1.36	2.51	1.54	55 nm
TaON	2.40	1.10	2.80	0.76	25 nm

Table 3: Dispersion data and layer thicknesses of the alternative tantalum nitride absorber.

SCHOTT Lithotec's three different mask blank types are all dry etch optimized. Sub 100 nm features like dense lines and spaces or contact holes have been successfully etched into the systems showing vertical side wall angles and high etch selectivity to the substrate. Especially the tantalum nitride alternative absorber offers the advantage of practically zero dry etch bias.

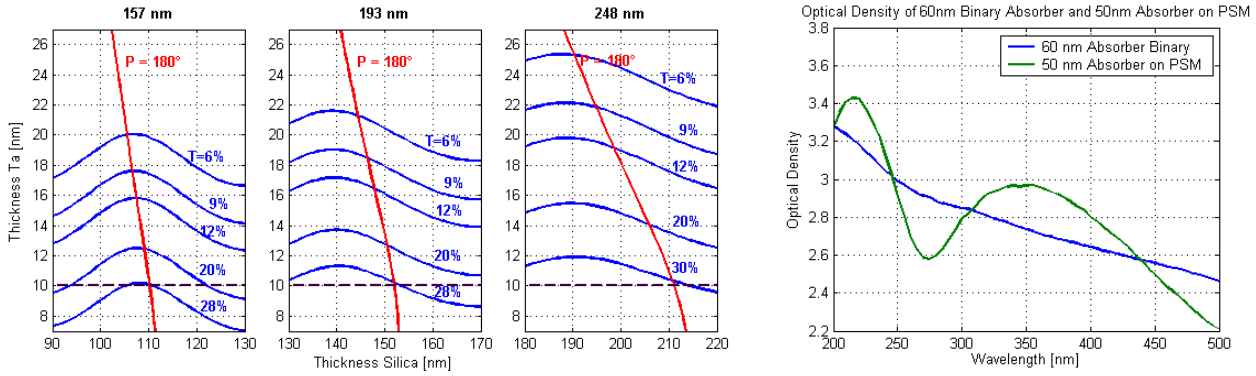

Figure 2: The Ta/SiO_2 PSM system can be adapted to three lithography wavelengths and transmission can be tuned up to 30% (left). The 50 nm chrome absorber has an optical density above 3 for wavelengths below 248 nm (right).

SCHOTT Lithotecs's two layer tantalum/silica phase shift system is very flexible. By thickness variations only the system can be tuned from 6% up to 30% transmission for 157, 193 and 248 nm lithography wavelengths as illustrated in Figure 2. Thus one film patterning process provides a wide product range. The variable transmission allows contrast tuning in lithographic processes and larger process windows can be obtained. The high etch stop capability of both the tantalum and silica layer yields improved CD and phase control. The absorber on top is either the 60 nm standard chrome absorber or an even thinner version of 50 nm only. The standard chrome absorber achieves an optical density above three for wavelengths below 248 nm with a layer thickness of 60 nm only. The right graph of Figure 2 compares the measured optical density of our 60 nm binary to the thickness optimized 50 nm PSM absorber. Optical density is above three below 248 nm for both systems. The binary chrome absorber has a significantly improved iso/dense bias.

3. MASK DESIGN AND FABRICATION

The mask blanks were patterned using a special design developed at the Advanced Mask Technology Center, Germany. The design consists of fields with an area of 4mmx4mm containing lines and spaces with a specified pitch size and duty cycle. The fields are separated by a distance of 1mm and arranged in a matrix with different fields corresponding to different pitches and line/pitch ratios.
All masks were patterned at the IMS Chips (Stuttgart, Germany) using new processes which provide sufficient uniformity and good pattern profiles. For all three masks a data correction was applied in order to obtain the targeted duty cycles. The structures were written into FEP171 resist using a Leica SB350, 50keV e-beam writer. Patterning of the chrome and tantalum-nitride absorbers was performed using standard dry etch processes. The two-layer halftone material (Ta/SiO2) was etched in a two-step process: first a fluorine based chemistry with etch stop on tantalum; second a chlorine based chemistry with etch stop on quartz.
For characterization of the mask features a Holon Secondary Electron Microscope (SEM) and a FEI Surface Nano Profiler (SNP) were used. The measured pitches are exact within 0.5%, whereas the duty cycle derived from SEM measurements should have an error less than 5%. For measurements of diffraction properties over pitch, structures with a line/pitch ratio of 0.5±0.01 (for binary mask materials) and 0.3±0.01 (for the phase shifter) were chosen. For more details on the actual design and the characterization of the masks we refer to [9].

4. EXPERIMENTAL SETUP

Determination of the optical layer properties by ellipsometry

Optical dispersion of the layers were determined at SCHOTT Lithotec by variable angle spectroscopic ellipsometry (VASE). Ellipsometry is a very sensitive and non-destructive method to determine optical properties of thin films by measuring the complex ratio between the parallel (p) and perpendicular (s) reflection coefficients $\rho = r_p / r_s = \tan \Psi \cdot \exp(i \cdot \Delta)$. The ellipsometric angles Ψ and Δ were acquired at three angles of incidence (55°, 65°, and 75°) over the spectral range of 145-1000 nm using a VUV-VASE® ellipsometer from J. A. Woollam Company. Intensity transmission data were also acquired with the VUV-VASE® at normal incidence over the same spectral range as the ellipsometric data.
Optical modeling and data analysis were done at SCHOTT Lithotec using the WVASE32™ software package from J. A. Woollam Company. Whereas the layer thicknesses determined by GIXR have been used as starting parameters, the ellipsometric data as well as the data on intensity transmission were fit simultaneously for all layer thickness series. This greatly helps in determining a unique optical model. Refractive index *n* and extinction coefficient *k* as the results of these simulations, can be found in tables Table 1 - Table 3, exemplarily for lithographic wavelength 193 nm and inspection wavelength 257 nm. These values, as well as the layer thicknesses, have been used as input parameters for the simulations based on rigorous coupled wave analysis (RCWA).

Measurements of the polarization dependant properties of the structured materials

The VUV-VASE® from J. A. Woollam Company was also used at SCHOTT Lithotec to measure the polarization dependent properties of the mask patterns, in particular the intensities in the 0^{th} and 1^{st} diffraction order for both polarization directions and varying angle of incidence (0°, 10°, and 20°). The experimental setup of this measurement

can be seen schematically in Figure 3. A Deuterium lamp including monochromator and polarizer is used to produce either TE- or TM-polarized light of 193 nm. Then the mask patterns are illuminated from the backside of the mask and the corresponding intensities of the 0^{th} and 1^{st} diffraction orders are measured with a photomultiplier tube detector. This detector is installed on a goniometer for continuous variation of the detector position. The mask holder offers to continuously vary the angle of incidence as well as the X- and Y-position of the mask to adjust to the correct pattern position.

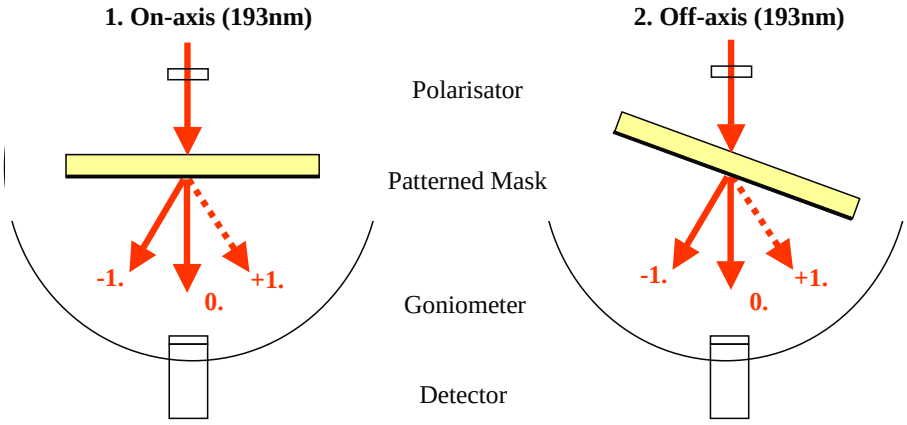

Figure 3: Schematic drawing of the degree of polarization measurement setup for a) on-axis b) off-axis.

5. RESULTS AND DISCUSSION OF POLARIZATION MEASUREMENTS

Fundamentals of Mask Polarization

In this paper we restrict ourselves to diffraction measurements of simple 1D-structures, i.e. lines and spaces with varying pitch and duty cycle. Lines and spaces with a half pitch corresponding to the critical dimension of the respective technology node are considered as critical features in high-end lithography. Furthermore, such a structure provides a suitable means to investigate mask topography effects, e.g. mask polarization. The underlying geometry is shown in Figure 4.

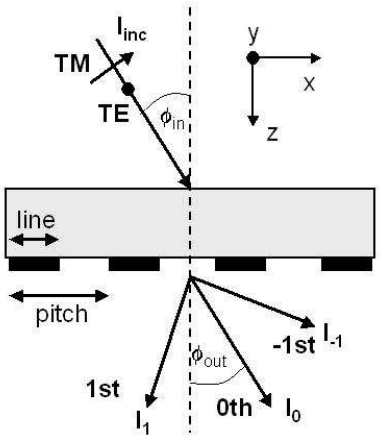

Figure 4: Diffraction of a plane wave incident upon diffraction grating.

The diffraction spectrum of an incoming plane wave with intensity I_{inc} is given by discrete orders m (m=…,-2,-1,0,1,2,…) with corresponding diffraction efficiencies η_m defined as

$$\eta_m = \frac{I_m}{I_{inc}} \ , \tag{1}$$

where I_m is the intensity of the m-th diffracted order. In a lithography system with small k_1, only the 0th and 1st order will enter the entrance pupil of the optical projection system and hence contribute to imaging. The polarization of an incoming wave is defined in Figure 4: a plane wave with an electric field vector parallel to the lines is referred to as transverse electric (TE) and a wave with an electric field perpendicular to the lines as transverse magnetic (TM). If the wavelength is small compared to the structures of the diffraction grating, the mask can be considered as infinitely thin, which is often referred to as the Kirchhoff approximation. If the structure size is in the order of a wavelength, efficiencies in the respective orders depend on pitch and on the actual cell structure, e.g. duty cycle, side wall angle, height etc. Furthermore, the diffraction efficiencies will be different for varying polarization of the incoming light. The polarization of a mask can be expressed in terms of the degree of polarization (DoP) defined as,

$$\mathrm{DoPm} = \frac{\eta_m^{TE} - \eta_m^{TM}}{\eta_m^{TE} + \eta_m^{TM}} \ , \tag{2}$$

where the upper index of η refers to TE- and TM-polarization, respectively. Due to field components in propagation direction, the image contrast is reduced for TM polarized light[3]. As the image obtained for unpolarized light is given by the incoherent superposition of both TE and TM components, the polarization of the mask can have a considerable impact on the imaging performance. A DoP of 1 in both orders can be considered as the optimum case for unpolarized light as no vector effects reduce the contrast.

In the following we compare intensities and mask polarization measured with the VUV-VASE® ellipsometer described in Section 4 with simulations based on material parameters described in Section 2. All simulations were performed using the commercially available diffraction grating analysis tool GSOLVER[10]. GSOLVER is based on rigorous coupled wave analysis providing an accurate solution of Maxwell's Equations. In all simulations, the efficiencies are calculated under the assumption of perfect structures, means lines with vertical sidewall angles. Whereas only diffraction on the top surface of the mask is taken into account, all simulations are corrected for by Fresnel losses at the bottom surface. It is further assumed that the shape of the light beam of the ellipsometer can be approximated by a plane wave.

Polarization Effects on Binary Materials

Figure 5 shows the DoP of binary materials versus mask pitch for lines and spaces with a fixed duty cycle of line/pitch=1:1. For the experimental verification, structures with a mask pitch down to 340nm were measured corresponding to a wafer CD of approximately 43nm. A good agreement between measurement and simulation can be observed.

For the chrome absorber, the DoP is small in the range from 1600 to 600nm (wafer CD 200nm-75nm). Below 600nm the DoP of the 1st order increases to approximately 0.15 at 360nm, means the mask polarizes light into the TE mode. This range is sometimes referred to as the waveguiding zone[4]. Note the existence of discontinuities at 380nm and 580nm, from which the latter is verified by the experimental data. This phenomenon is known as Wood's Anomalies and can be related to the emergence of higher diffracted orders, here the 2nd and 3rd orders, respectively[11,12,7].

For the tantalum nitride absorber the DoP of the 0th order is negative with increasing TM polarization down to 440nm, whereas in the1st order the diffraction efficiency for TE is slightly larger than for TM. Again, a sharp peak due to resonance effects appears at mask pitch=2λ. Comparing both binary materials it is observed that for a mask pitch of 400nm corresponding to a CD of 50nm the tantalum nitride absorber with an overall layer thickness of 80nm supports TM polarization, whereas the chrome absorber with a thickness of 60nm shows increased transmission for TE polarization.

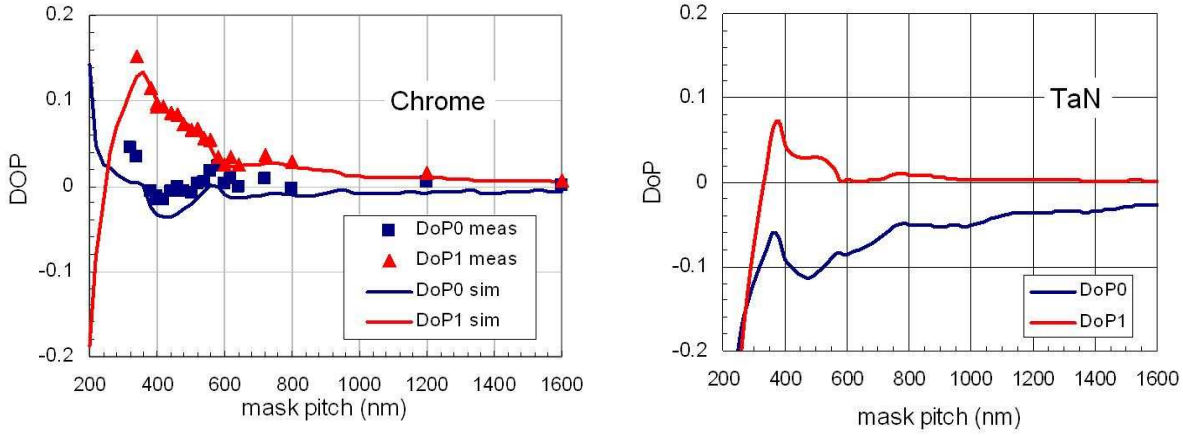

Figure 5: Degree of Polarization versus mask pitch for chrome absorber and tantalum nitride absorber: comparison between measurement and simulation.

In a further experiment, we investigated the transmission of binary masks for varying duty cycle at a fixed mask pitch of 400nm corresponding to a wafer CD of 50nm. In Figure 6 the intensities in the respective diffraction orders are shown for the chrome absorber. Again, there is a good agreement between measurement and simulation. The normalized mask transmission in the 0^{th} order amounts to approximately 0.2 at line/pitch=1:1. A significant difference in transmission between TE and TM polarized light is observed in the first order with maximum TE transmission of around 0.09 at a duty cycle of 0.48. As shown in Figure 7, this leads to a DoP0 of around 0.1 in the relevant duty cycle range of 0.4-05. Also depicted in Figure 7 is the polarization at an angle of incidence of 20°. With increasing angle the mask is polarized more TE resulting in a DoP1 of around 0.2. This is also shown in Figure 9, where polarization is plotted against the angle of incidence for both binary materials.

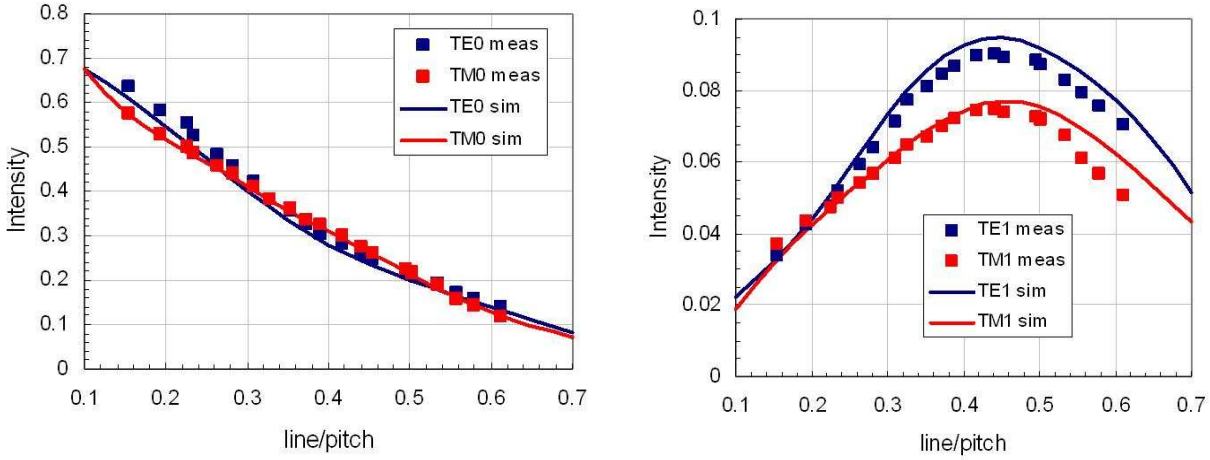

Figure 6: Normalized intensities in diffraction orders versus duty cycle (ϕ_{inc}=0) for chrome absorber at mask pitch 400nm: comparison between measurement and simulation.

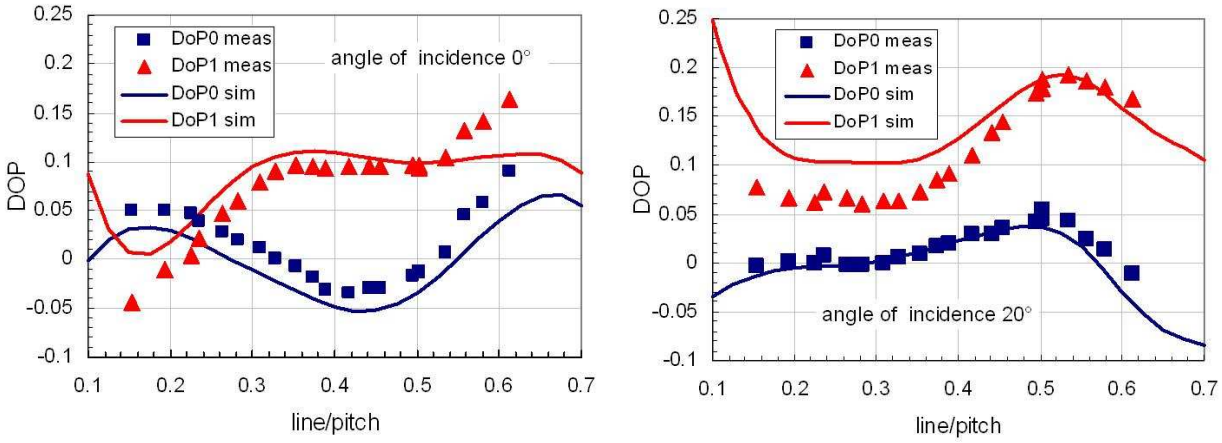

Figure 7: Degree of polarization versus duty cycle for chrome absorber at mask pitch 400nm for varying angle of incidence: comparison between measurement and simulation.

In Figure 8 transmission and polarization versus duty cycle are shown for the patterned tantalum nitride absorber. The maximum transmission in the 1st order of 0.11 is found at a duty cycle of around 0.38. Note that TaN shows smaller intensities in the 0th order and larger intensities in the 1st order compared to the chrome material. As will be discussed later this can lead to a larger contrast for duty cycles in the relevant range 0.35-0.5. The polarization in this range is predominantly TM in the 0th order and TE in the first order with a DoP of around –0.1 and 0.1, respectively. As indicated in Figure 9, the angle dependency of polarization is smaller than for the chrome absorber.

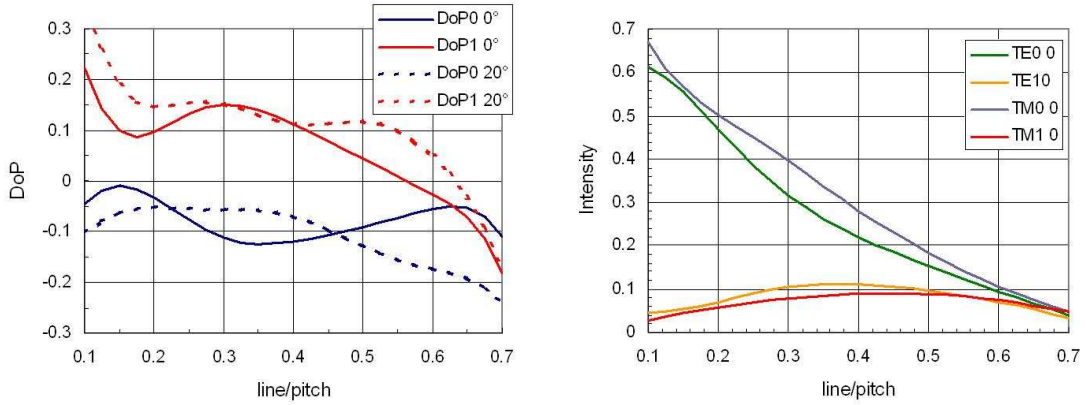

Figure 8: Degree of polarization and intensities in diffraction orders versus duty cycle for tantalum nitride absorber at mask pitch 400nm (vertical incidence): comparison between measurement and simulation.

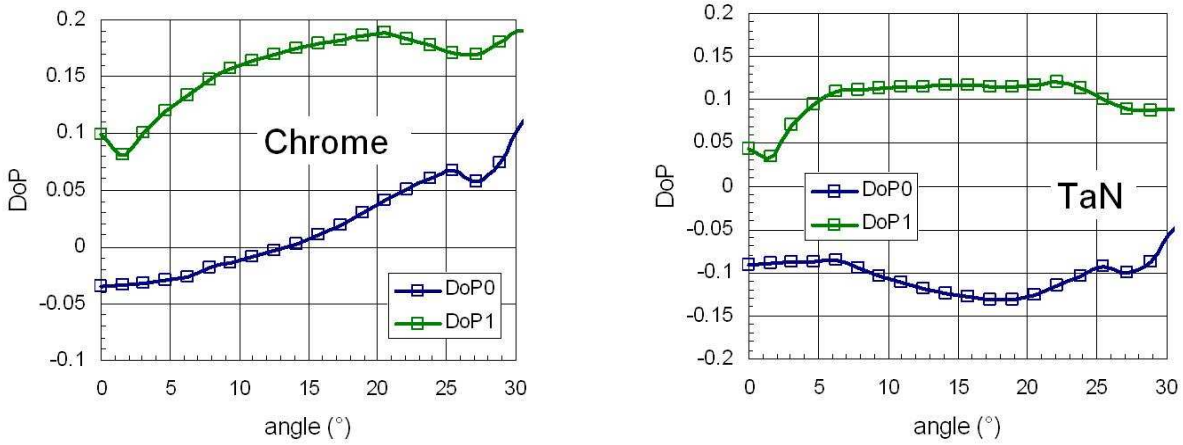

Figure 9: Degree of polarization versus angle of incidence at mask pitch 400nm and line/pitch=1:1 for chrome absorber and tantalum nitride absorber: comparison between measurement and simulation.

Polarization Effects on Phase Shifting Material

The polarization properties of the tantalum/silica material system are depicted in Figure 10 and Figure 11. As the optimum pattern bias for the material system is at a duty cycle of line/pitch=0.2-0.3 (see also next subsection), for an investigation of diffraction properties over pitch we choose a duty cycle of line/pitch=0.3. As can be seen in Figure 10, the phase shifter shows complex polarization properties with the 0^{th} order mainly TM polarized and the 1^{st} order predominantly TE polarized. For pitches smaller than 400nm, there is a sharp decrease in efficiency for TE in the 0^{th} order. At a mask pitch of 400nm, large differences in efficiencies between TE and TM can be observed for all relevant duty cycles. As illustrated in Figure 11, this leads to a DoP of around -0.2 in the 0^{th} order and 0.2 in the 1^{st} order for line/pitch=0.15-0.35 at vertical incidence. Also shown here is the rather strong influence of the angle of incidence on polarization, which leads mainly to an increasing TM polarization in the 0^{th} order. Compared to the binary material system, the phase shifter shows larger polarization effects with a strong dependence on pitch, duty cycle and angle of incidence.

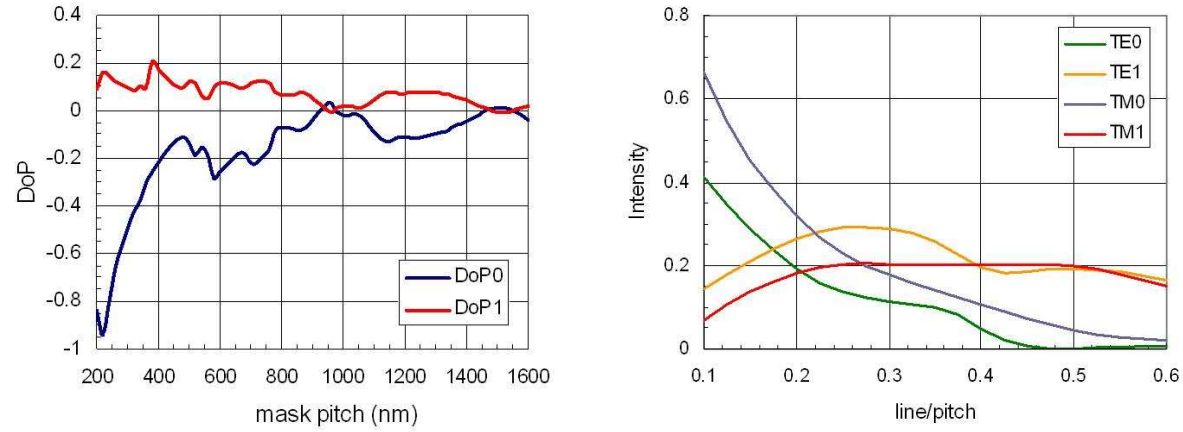

Figure 10: Degree of polarization versus mask pitch for phase shifter with duty cycle line/pitch=0.3: comparison between measurement and simulation (right); Normalized intensities versus duty cycle for mask pitch 400nm, vertical incidence (left).

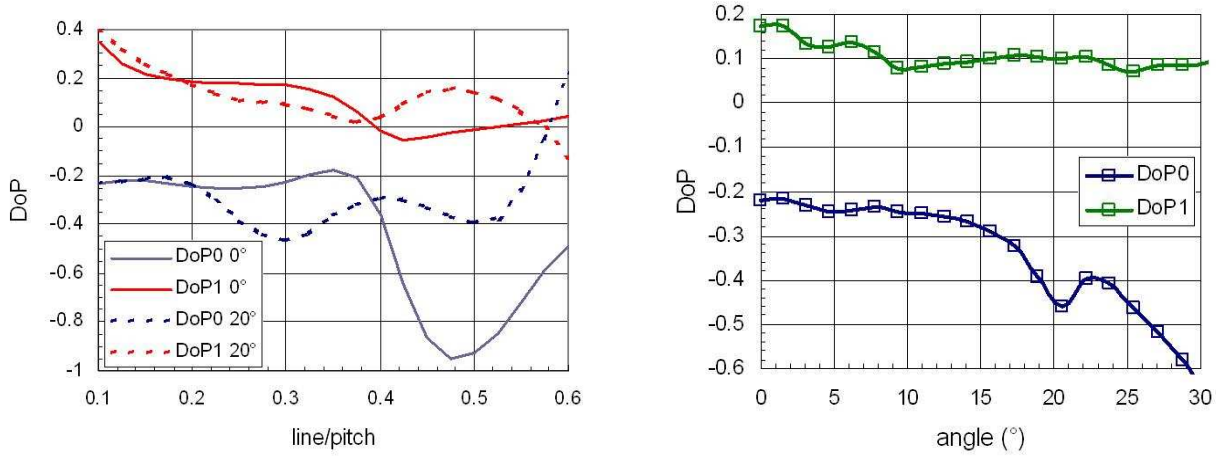

Figure 11: Degree of polarization versus duty cycle for phase shifter at mask pitch 400nm for angle of incidence 0° and 20°, respectively (right); Degree of polarization versus angle of incidence at mask pitch 400nm and line/pitch=0.3 (left).

Influence of Polarization on Imaging Properties

Up to now, the diffraction properties of the respective mask types were mainly described in terms of the degree of polarization. However, it is useful to elaborate more on the influence of mask polarization on the lithographic performance. Because a detailed examination of imaging properties of masks is beyond the scope of this paper, the influence of polarization is estimated by means of the image contrast obtained from simple two-beam interference. Comparing these calculations with results obtained with the Kirchhoff approximation gives a rough estimate of the effect of redistribution of light between the diffraction orders.
Referring to Figure 4, the mask is illuminated with a plane wave at an angle corresponding to optimal dipole illumination, i.e.,

$$\sin(\phi_{\text{in}}) = \frac{\lambda}{2p} \ , \tag{3}$$

where p is the mask pitch. Neglecting polarization effects at the water/resist surface, the contrast for unpolarized illumination obtained from two-beam interference is given by,

$$\text{contrast} = 2\frac{\sqrt{\eta_0^{\text{TE}}\eta_1^{\text{TE}}} + c_\alpha\sqrt{\eta_0^{\text{TM}}\eta_1^{\text{TM}}}}{\eta_0^{\text{TE}} + \eta_1^{\text{TE}} + \eta_0^{\text{TM}} + \eta_1^{\text{TM}}} \ , \tag{4}$$

where the factor c_α describes the reduced contrast due to TM-polarization,

$$c_\alpha = \cos^2(\alpha) - \sin^2(\alpha), \ \sin(\alpha) = \frac{\lambda}{2pn_{\text{R}}} \ , \tag{5}$$

with n_R=1.7 is the refractive index of the resist. In the following the image contrast according to Eq. (4) is calculated from diffraction efficiencies obtained with GSOLVER based on the material parameter in Section 2. In the Kirchhoff approach the diffraction efficiencies are not dependent on polarization ($\eta_m^{TE}=\eta_m^{TM}$) and can be calculated analytically[8]. A common assumption for the simulation of aerial images is the Hopkins-approximation. Here it is assumed that the diffraction efficiencies under oblique incidence are equal to the case of perpendicular illumination, whereas diffraction orders are shifted in the entrance pupil depending on the incidence angle of the incoming plane wave. For Hyper NA systems, this assumption might not be valid anymore. As shown in the previous subsection, the intensities in the different orders are indeed dependent on the angle of incidence. To estimate angular effects on the contrast, Eq. (4) is also calculated for diffraction orders obtained at perpendicular incidence.

Figure 12 shows the simulated image contrast for the chrome absorber versus duty cycle for a mask pitch of 400nm. The contrast predicted from rigorous calculations is larger than the one obtained for a Kirchhoff-mask. The differences between calculations with efficiencies obtained with perpendicular and oblique incidence are rather small.

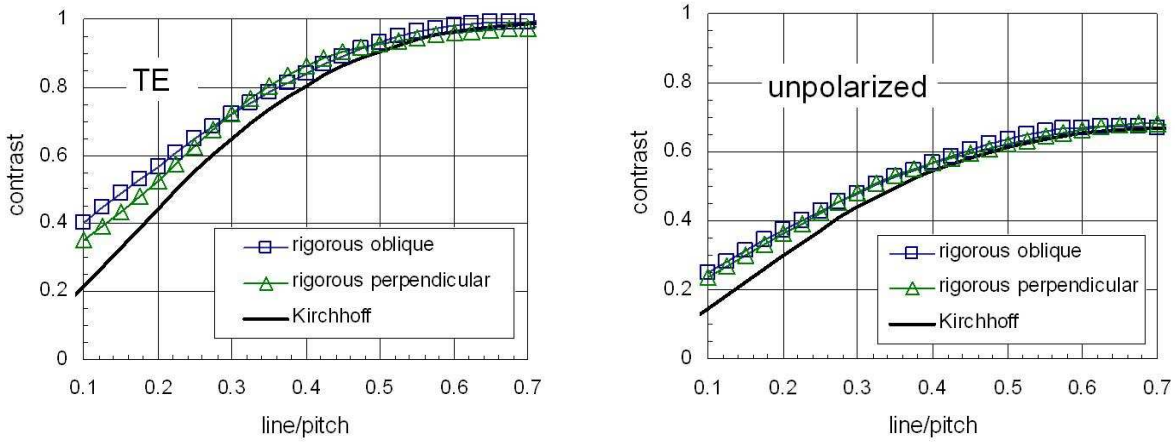

Figure 12: Simulated contrast versus duty cycle at mask pitch 400nm for chrome absorber for TE polarization and unpolarized light.

A comparison between both binary materials is shown in Figure 13. As indicated in Figure 8, the decreased difference between 0^{th} order and 1^{st} order for the tantalum nitride absorber results in a larger contrast at a given duty cycle compared to chrome. For unpolarized illumination, the maximum contrast for tantalum nitride is slightly smaller indicating the influence of TM polarization of the mask.

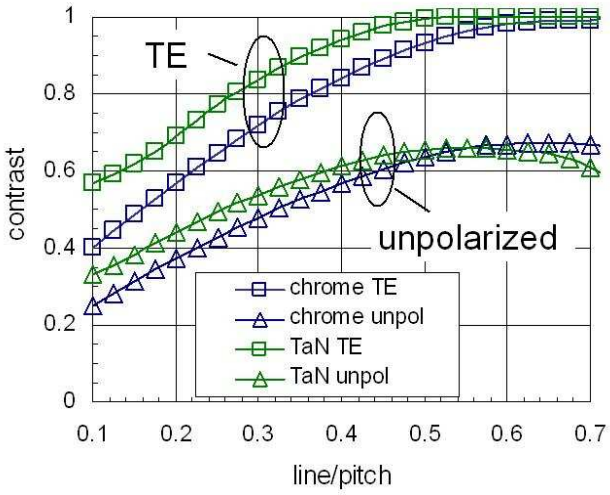

Figure 13: Comparison between chrome absorber and tantalum nitride absorber: contrast versus duty cycle.

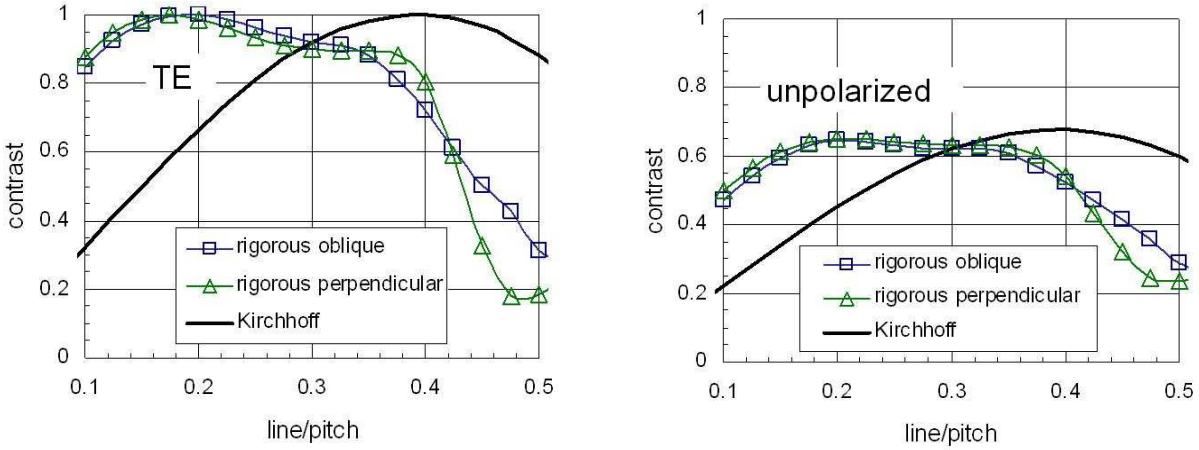

Figure 14: Simulated contrast versus duty cycle for tantalum/silica phase shifter: TE polarization and unpolarized light.

For the tantalum/silica phase shifter the differences between Kirchhoff-approximation and rigorous calculations are even more severe. The optimum duty cycle is shifted from line/pitch=0.4 to a value of 0.2. The contrast exhibits a large plateau for duty cycles from around 0.15 to 0.35 for both TE polarization and unpolarized light. Strong angular effects are observed in the range greater than 0.35. Optimum contrast for unpolarized light is slightly smaller than predicted for a Kirchhoff-mask indicating the influence of polarization.

A summary of results obtained for unpolarized light is given in Table 4. The contrast for binary materials is compared at line/pitch=0.5, for the phase shifter the maximum contrast is given. The contrast for binary materials is increased whereas the high transmission material shows a slightly smaller contrast due to polarization. However, the effect is rather small. This can be attributed to the fact that the DoP in the 0^{th} order and 1^{st} order have different signs resulting in a cancellation effect.

Material	RCWA				Kirchhoff	
	contrast	line/pitch	DoP0	DoP1	contrast	line/pitch
Chrome	0.64	0.5	0	0.17	0.61	0.5
TaN	0.65	0.5	-0.12	0.12	0.61	0.5
Ta/Si phase shifter	0.65	0.2	-0.24	0.2	0.68	0.4

Table 4: Contrast calculated from two beam interference for unpolarized light: comparison between RCWA and Kirchhoff-approximation.

6. CONCLUSIONS

Three new mask materials developed at Schott Lithotec have been investigated with respect to polarization properties. These are two binary absorbers based on chrome and tantalum nitride as well as a phase shifter based on tantalum/silica. Material properties were measured using grazing incidence x-ray reflectometry (GIXR) and variable angle spectroscopic ellipsometry (VASE), and respective material data are given. All masks were patterned with dense lines and spaces with varying pitches and duty cycles. The diffraction spectrum was measured with VASE and compared with simulations based on RCWA. Both simulation and experiment show good agreement indicating that the materials are well characterized.

All materials show complex polarization properties depending on pitch, line width and angle of incidence. At a mask pitch of 400nm (corresponds to 50nm halfpitch on wafer), the chrome absorber polarizes mainly into TE whereas the tantalum absorber shows TM polarization. Largest polarization effects are observed for the phase shifter with the 0^{th} order mainly TE and the 1st order mainly TM-polarized. A contrast estimation based on two-beam interference shows the influence of topography effects like polarization but does not give an indication that the materials cannot be used at the 50nm node.

ACKNOWLEDGEMENTS

The authors would like to thank Ralf Ziebold at INFINEON Technologies for fruitful discussions. This reasearch was supported by the German Federal Ministry of Education and Research (BMBF) under contract No. 01M3154A ("Abbildungsmethodiken für nanoelektrische Bauelemente").

REFERENCES

1. A. K. Wong, "Resolution Enhancement Techniques in Optical Lithography", SPIE Press, 2001.
2. B. Streefkerk, et al., "Extending Optical Lithography with Immersion", *Proceedings of the SPIE*, vol. 5377, pp. 285-305, 2004.
3. B. W. Smith, J. Cashmore, "Challenges in high NA, polarization, and photoresists", *Proceedings of the SPIE*, vol. 4691, pp. 11-24, 2002.
4. D. G. Flagello, et al., „Optical lithography in the sub-50nm regime", *Proceedings of the SPIE*, vol. 5377, pp. 21-33, 2004.
5. B. W. Smith, L. Zavyalova, and A. Estroff, „Benefitting from polarization-effects on high-NA imaging", *Proceedings of the SPIE*, vol. 5377, pp. 68-79, 2004.
6. B. J. Lin, "Immersion lithography and its impact on semiconductor manufacturing", *Proceedings of the SPIE*, vol. 5377, pp. 46-65, 2004.
7. A. Estroff, et al., „Mask induced polarization", *Proceedings of the SPIE*, vol. 5377, pp. 1069-1080, 2004.
8. A. Erdmann, "Mask Modeling in the Low K1 and Ultrahigh NA Regime: Phase and Polarization Effects", to be published.
9. S. Teuber, et al., „Determination of mask induced polarization effects ocurring in hyper NA immersion lithography", to be published.
10. GSOLVER Product Site, http://www.gsolver.com
11. R. W. Wood, "Uneven Distribution of Light in a Diffraction Grating Spectrum", Philosophical Magazine, September 1902.
12. Lord Rayleigh, "On the remarkable Case of Diffraction Spectra Described by Prof. Wood", Philosophical Magazine, July, 1907.